Impact of the sleeve thickness on the armature eccentricity in a solenoid valve

ROBERT GORAJ

Paul Gossen Str. 99, 91052 Erlangen, Germany
e-mail: robertgoraj@gmx.de

Abstract: Most studies on solenoid valves (SVs) assumed that the armature is concentrically positioned in the sleeve. Under this assumption the transversal component of the magnetic force is equal zero. The article presents an analytical calculation model for the estimation of the armature eccentricity. Using this model the eccentricity was calculated as a function of the sleeve thickness and the hydraulic clearance between the armature and the sleeve. After finding the eccentricity also the permeance of the radial air gap was calculated. This permeance has a direct influence on the drop of the magnetomotive force in the magnetic circuit and finally influences also the axial component of the magnetic force. In the article a calculation of both transversal and axial components of the magnetic force was carried out and presented in the appendix to the article.

Key words: solenoid valve, eccentricity, armature, sleeve

1. Introduction

Nowadays SVs are studied in the early stage of system development. Most of these studies focus on the modeling, dynamic response and control method of SVs. There are lots of reports regarding finite-element approaches [1], simulation models [2] and control [3, 4] of SVs as well as investigation of temperature distribution and thermal deformations inside the SV [5]. One can also find reports regarding the electromagnetic driving force of SV. The driving force is the force acting in the direction of the solenoid axis extending along the longitudinal length of the armature. In [6] authors presented a research of key parameters influencing the driving electromagnetic force of a SV. The driving force causes the movement of the SV armature and decreases the axial magnetic gap. In conventional linear solenoids the armature slides during its movement on the inner surface of the sleeve. The sleeve is usually made from a paramagnetic material e.g. an aluminum alloy. The objective of the usage of a paramagnetic material is the insertion of the second magnetic gap in the magnetic circuit. This gap is placed between the armature and the magnet yoke and is denoted as the radial magnetic gap (Fig. 1). In most studies on SVs the thickness of the radial gap is kept constant independent from the circumferential angle. In other words researchers take an assumption that the armature is placed concentrically in the sleeve. This assumption implies the homogeneous distribution of radial

magnetic forces over the armature circumference. Because of e.g. manufacturing imperfections the armature is in fact positioned eccentrically in the sleeve. In this case the distribution of radial magnetic forces over the armature circumference isn't homogeneous and the resulting radial magnetic force attracts the armature toward the nearer side of the pole. Thus, an increased transverse force acting on the armature exists and causes friction between the armature and the sleeve. Friction with these components degrades the performance of the solenoid and causes wear. The investigation of the transverse magnetic force has been rarely reported. Sophisticated numerical computations by means of a 2D finite difference method ware carried out in [7]. One can also find some inventions having an objective to minimize the transverse force that occurs from armature eccentricity. In [8] the author described the reduction of the transverse force by the introduction of segmentation in the armature member. In [9] the transverse force is minimized by the insertion of small radial slots in the armature side surface. The objective of the study is to investigate which impact has the thickness of the sleeve on the eccentricity of armatures with different radii.

2. Hydraulic and magnetic radial gaps

The investigated solenoid valve was simplified to the layout shown Fig 1. The inner cylinder (with the radius r_1) is the cross section of the solenoid valve armature. The room between the radii r_1 and r_2 is filled with oil. The ring between the radii r_2 and R_3 is the cross section of the solenoid valve sleeve.
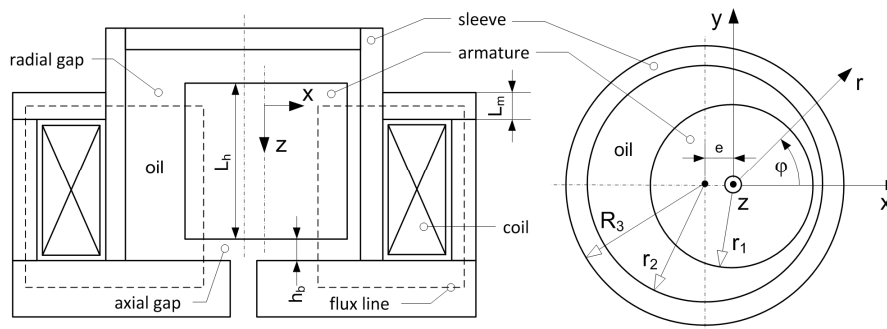

Fig. 1. Simplified layout of the solenoid valve

The difference between the inner radius of the sleeve and the radius of the armature is defined as the hydraulic clearance δ_h. The difference between the outer radius of the sleeve and the radius of the armature is defined as the nominal radial magnetic gap δ_m.

$$\delta_h = r_2 - r_1,$$ (1)

$$\delta_m = R_3 - r_1.$$ (2)

The thickness of the sleeve is the difference of its outer and inner radius

$$\delta_u = R_3 - r_2 . \tag{3}$$

The eccentricity of the armature e is defined as a radial offset between the sleeve and the armature axis (Fig. 1. on the right). Analogously to this definition follow definitions of the relative hydraulic and the magnetic eccentricities

$$\varepsilon_h = e\delta_h^{-1}, \tag{4}$$

$$\varepsilon_m = e\delta_m^{-1} . \tag{5}$$

Position-dependent hydraulic and magnetic gaps can be simplified for $\delta_h << r_1$ and $\delta_m << r_1$ to [10]

$$h_h = \delta_h\left(1 - \varepsilon_h \cos\varphi\right), \tag{6}$$

$$h_m = \delta_m\left(1 - \varepsilon_m \cos\varphi\right). \tag{7}$$

3. Permeance of axial and radial gap

The permeance of the axial gap can be found using the formula that describes the room between two parallel surfaces with the area A_d [11]

$$G_1 = \mu_0 A_d h_b^{-1} . \tag{8}$$

The physical quantity μ_0 in (8) is the permeability of vacuum. In the model it is assumed that the permeability of the oil, the solenoid valve is filled with and the permeability of the sleeve are equal to the permeability of the vacuum. In the case of armatures with axial holes the cross section A_d is smaller than the area of the top of the cylinder shown in Fig. 1. The axial holes have cylindrical form and are used for the mass reduction. An example of such holes can be seen in [9]. For such armatures in the case of a given radius $r_1 = R_1$ the cross section A_d is equal to A_d^0. Because the upcoming calculations are not restricted to the single armature radius but the calculations are going to be performed for different armature radii the area A_d can be determined as

$$A_d = A_d^0 + \pi\left(r_1^2 - R_1^2\right). \tag{9}$$

The setting of (9) in (8) yields the permeance of the axial gap

$$G_1 = \mu_0\left(A_d^0 + \pi(r_1^2 - R_1^2)\right)h_b^{-1} . \tag{10}$$

The parameter h_b in (10) is the length of the axial magnetic gap (Fig. 1). The permeance of the room between cylinders placed eccentrically in one another can be approximated using [11]

$$G_2 = \mu_0 2\pi r_1 L_m \left(\delta_m^2 - e^2\right)^{-1/2} . \tag{11}$$

The parameter L_m in (11) is the width of the yoke pole (Fig. 1). Changing in (11) the absolute armature eccentricity with the relative eccentricity (5) yields

$$G_2 = \mu_0 2\pi r_1 L_m \delta_m^{-1} \left(1 - \varepsilon_m^2\right)^{-1/2} . \tag{12}$$

The formulas (8) and (12) will further be used in the calculation of the magnetic flux density in the axial and in the radial gaps.

4. Magnetic flux density

For the calculation of the magnetic flux density it is assumed that in the considered system the magnetomotive force θ is constant

$$\theta = Ni . \tag{13}$$

The parameter N in (13) is the number of coil windings and i is the value of electrical current flowing in the coil. It is also assumed that all metallic materials which participate in the building of the magnetic circuit have the infinite high permeability. Furthermore it is assumed that in the axial gap the magnetic flux density has only the axial component and it is spatially homogenously distributed

$$\mathbf{B}_1 = (B_1^r, B_1^\varphi, B_1^z)^T = \mathbf{e}^z B_1^z . \tag{14}$$

Under this set of assumption one obtains the magnetic flux ϕ after a multiplication of B_1^z with the armature top area (9)

$$\phi = B_1^z \left(A_d^0 + \pi(r_1^2 - R_1^2)\right). \tag{15}$$

In the radial gap the magnetic flux density is distributed over the armature circumference. In the case of a tight slot for which $\delta_m \ll r_1$ it can be assumed that the magnetic flux density in the radial gap has only the radial component

$$\boldsymbol{B}_2 = (B_2^r, B_2^\varphi, B_2^z)^T = \boldsymbol{e}^r B_2^r(\varphi) . \tag{16}$$

Under the use of the Ampère's circuital law [12] one obtains under the previously taken assumptions

$$B_1^z h_b + B_2^r h_m = \mu_0 \theta . \tag{17}$$

The use of the Hopkinson's law [13] yields

$$\phi G_1^{-1} + \phi G_2^{-1} = \theta . \tag{18}$$

The permeances G_1 and G_2 come from the formulas (10) and (12) respectively. After solving the equation system (10), (12), (15), (17), (18) one finally obtains the components of the magnetic flux densities in the axial and in the radial gap

$$B_1^z = \mu_0 \frac{\theta}{h_b} \frac{G_2}{G_1 + G_2} , \qquad (19)$$

$$B_2^r(\varphi) = \mu_0 \frac{\theta}{h_m} \frac{G_1}{G_1 + G_2} . \qquad (20)$$

The formulas (19) and (20) will be used in the computation of the magnetic force acting on the armature of the solenoid valve.

5. Magnetic force

Under the assumption taken in the previous section the resulting magnetic force acting on the armature can be estimated using [14]

$$\mathbf{F}_m = \left(F_m^x, F_m^y, F_m^z\right)^T = (2\mu_0)^{-1} \oiint_A B^2 d\mathbf{A} . \qquad (21)$$

In the case of the axial component of the magnetic force the integration of (19) over the top surface of the armature is obvious and the formula (21) simplifies to

$$F_m^z = p_{m1} A_d . \qquad (22)$$

The physical quantity p_{m1} in (22) is the density of the magnetic energy [15]

$$p_{m1} = (2\mu_0)^{-1} \left(B_1^z\right)^2 . \qquad (23)$$

After the setting of (23), (19) and (9) in (22) one obtains

$$F_m^z = \frac{\mu_0}{2} \left(\frac{\theta}{h_b} \frac{G_2}{G_1 + G_2} \right)^2 \left(A_d^0 + \pi(r_1^2 - R_1^2)\right). \qquad (24)$$

For the estimation of the transverse magnetic force one needs first a definition of the vectorial surface element. It is given in the coordinate-system x, y (Fig. 1) with

$$d\mathbf{A} = r_1 d\varphi dz (\cos\varphi, \sin\varphi, 0)^T . \qquad (25)$$

Because of the symmetry reason the transverse magnetic force has in the coordinate-system x, y only the x-component. The integration of (20) in z-direction in boundaries $z \in \langle 0, L_m \rangle$ yields

$$F_m^x = r_1 L_m \int_0^{2\pi} p_{m2} \cos\varphi \, \mathrm{d}\varphi \,, \tag{26}$$

with physical quantity p_{m2} equal to

$$p_{m2}(\varphi) = (2\mu_0)^{-1}(B_2^r)^2 \,. \tag{27}$$

After the setting of (27), (20) and (7) in (26) one obtains

$$F_m^x = \frac{\mu_0}{2} \left(\frac{\theta}{h_m} \frac{G_1}{G_1+G_2} \right)^2 L_m r_1 \int_0^{2\pi} \cos(\varphi)(1-\varepsilon_m \cos(\varphi))^{-2} \, \mathrm{d}\varphi \,. \tag{28}$$

The integral in (28) can be expressed as follows

$$J_2^{01} = \left[I_2^{01} \right]_0^{2\pi} = \int_0^{2\pi} \cos(\varphi)(1-\varepsilon_m \cos(\varphi))^{-2} \, \mathrm{d}\varphi \,. \tag{29}$$

The solution to (29) was found using the integral tables [16] and is described in the appendix A. The integral (29) is equal

$$J_2^{01} = 2\pi\varepsilon_m \left(1-\varepsilon_m^2\right)^{-3/2} \,. \tag{30}$$

The setting of (30) in (28) yields the x-component of the magnetic force

$$F_m^x = \mu_0 \pi \left(\frac{\theta}{\delta_m} \frac{G_1}{G_1+G_2} \right)^2 \frac{\varepsilon_m}{\left(1-\varepsilon_m^2\right)^{3/2}} L_m r_1 \,. \tag{31}$$

The x-component of the magnetic force is in the considered case equal to the transversal magnetic force. It stays in equilibrium with the contact force between the armature and the sleeve.

6. Contact force of the armature

The reaction to the transverse magnetic force is the contact force. It can be estimated by integrating the contact pressure p_k over the armature side surface

$$\mathbf{F}_k = \left(F_k^x, F_k^y, F_k^z \right)^T = -\oiint_A p_k \, \mathrm{d}\mathbf{A} \,. \tag{32}$$

One obtains the contact pressure using the pressure model of Greenwood-Williamson [17]

$$p_k = \pi \frac{16}{15} \sqrt{2} (m_R \beta \sigma)^2 E' \sqrt{\frac{\sigma}{\beta}} 3.48 \cdot 10^{-5} \left(4 - \frac{h_h}{\sigma} \right)^{7.05} (1 - \chi) . \tag{33}$$

The number of contact peaks per surface unit m_R the curvature radius β of contact peaks and the roughness σ aren't independent of each other. It can be assumed that $m_R \beta \sigma = 0.5$ [10]. The physical quantity E' is the reduced module of elasticity of the contact armature-sleeve. The function χ is the Heaviside's function with the argument $h_h(4\sigma)^{-1}$. The use of the vectorial surface element (25) and integration in $z \in \langle 0, L_h \rangle$ yields the *x*-component of the contact force

$$\mathbf{F}_k = \left(F_k^x, F_k^y, F_k^z \right)^T = -\oiint_A p_k \, \mathrm{d}\mathbf{A} . \tag{34}$$

The parameter L_h in (34) is the axial length of the armature (Fig. 1). The integration over φ was done using numerical methods.

7. Calculation results

The transverse magnetic force (31) and the contact force (34) stay in equilibrium with one another and both depend on the armature eccentricity. One obtains the armature eccentricity as the solution to the equation (35)

$$F_m^x(e) + F_k^x(e) = 0 . \tag{35}$$

The Equation (35) was solved numerically for different armature radii r_1 and different inner sleeve radii r_2 (Fig. 1). The outer radius of the sleeve R_3 was kept constant in the calculation. The calculation ranges are indicated by (36) and (37)

$$r_1 \in \left\langle R_1, R_3 - \delta_m^{\min} \right\rangle , \tag{36}$$

$$r_2 \in \left\langle r_1 + \delta_h^{\min}, R_3 - \delta_m^{\min} + \delta_h^{\min} \right\rangle . \tag{37}$$

One can recognize from (37) that the lower border of the radius r_2 depends on the radius r_1. Because of this dependency the calculation room isn't a square but it becomes a triangle. Restrictions of the ranges (36) and (37) are listed in the Table 1.

Table 1. Geometrical parameters of armature and sleeve

Parameter	Value	Unit
$2R_1$	11.5	mm
$2R_3$	12.1	mm
$\delta_m^{\min}$	150	μm
$\delta_h^{\min}$	10	μm

In the investigated case the value of the roughness of the contact armature-sleeve is $\sigma = 0.5$ µm. The calculated armature eccentricity was shown as a function of the sleeve thickness δ_u and the hydraulic clearance of the armature δ_h according to (3) and (1) in Fig. 2 on the left. One can see from this figure that the armature eccentricity strongly depends on the hydraulic clearance. The value of the armature eccentricity in the whole calculation range is about 1 µm less that the value of the hydraulic clearance. From this view one cannot however recognize any dependency on the sleeve thickness.
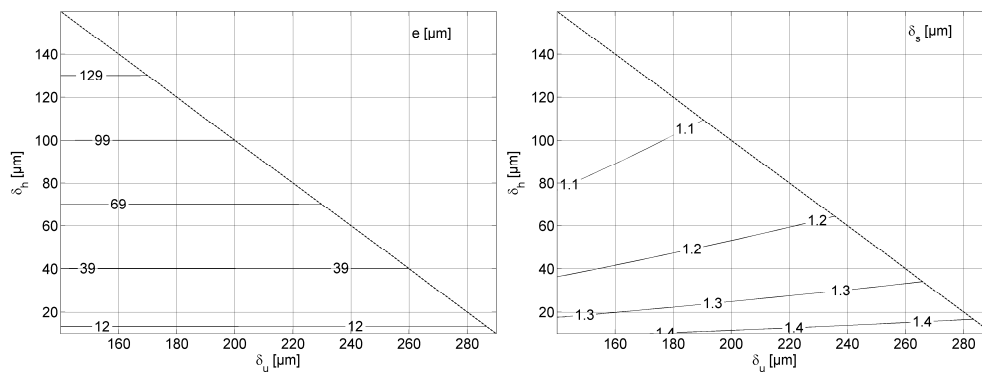
Fig. 2. Absolute armature eccentricity (left) and minimum distance from armature side surface to inner sleeve surface

In order to recognize this dependency the minimum distance from the armature side surface to the inner sleeve surface according to

$$\delta_s = r_2 - r_1 - e,\qquad(38)$$

was shown in Fig. 2 on the right. This distance varies in the whole calculation range from about 1 µm to about 1.5 µm. The increase of the sleeve thickness from 140 µm to 290 µm (for $\delta_h = 10$ µm) results in the increase of δ_s of about 0.1 µm. The reason for this increase is the transversal component of the magnetic force that lowers its value for big sleeve thickness δ_u. In this case the armature is attracted less intensively to the sleeve. The magnetic force acting on the armature, the magnetic flux and the magnetic permeance are shown in the appendix B.

The relative hydraulic and the magnetic eccentricities according to (4) and (5) are shown in Fig. 3. The maximal and the minimal values of these eccentricities aren't clearly recognizable in Fig. 3. The relative hydraulic eccentricity varies in the calculation range from about 85% to about 99%. Similarly to the absolute eccentricity e, also ε_h is almost independent of the sleeve thickness δ_u and strongly dependent on the hydraulic clearance δ_h. The relative magnetic eccentricity ε_m varies in the calculation range from about 3% to about 53%. Its dependence of the sleeve thickness becomes higher for big hydraulic clearances.

Another way to visualize the impact of the sleeve thickness on the armature eccentricity is to show δ_s (38) as a shoal of one dimensional functions $\delta_s = f(\delta_u)$ for some selected constant values of r_1-R_1.
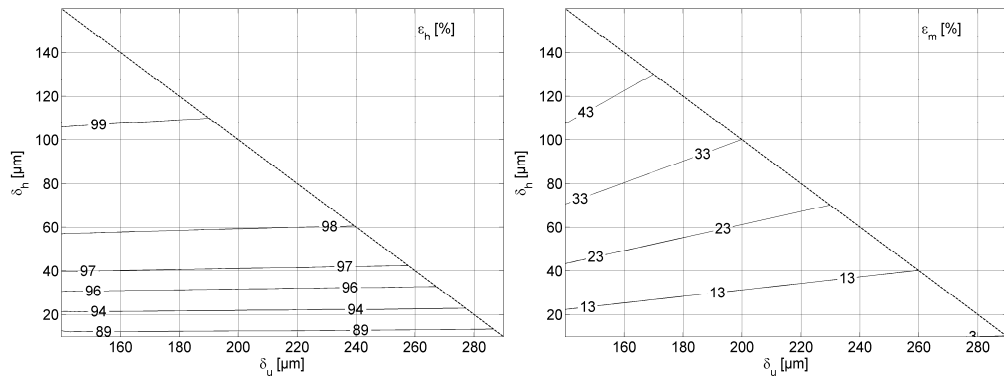
Fig. 3. Relative hydraulic (left) and relative magnetic eccentricity of the armature

For visualisation purposes nine constant values in the range of $r_1 - R_1 \in \langle 0, 133 \rangle$ µm was chosen. The distance δ_s is showed in Fig. 4 on left. The current value of r_1-R_1 is indicted on the top of Fig. 4. One can see from this figure that the impact of δ_u on δ_s is stronger for big armature radii. The increase of δ_u from 140 µm to about 160 µm caused the decrease of e to about 0.15 µm for $r_1 = R_1 + 133$ µm while the same increase of δ_u but in the case of $r_1 = R_1$ caused the decrease of *e* of only about 0.04 µm.
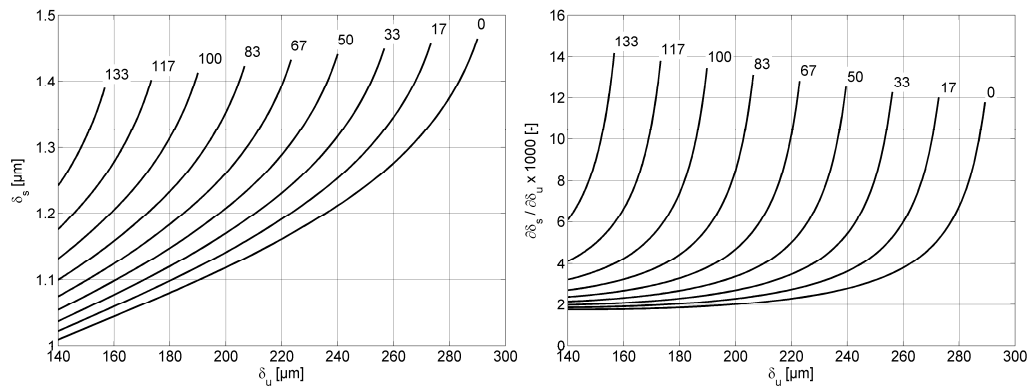

Fig. 4. Shoal of minimum distances from the armature side surface to the inner sleeve surface (left) and shoal its derivative

In order to visualize the impact of the sleeve thickness on the armature eccentricity the shoal of the derivatives $\partial \delta_s / \partial \delta_u$ was plotted in Fig. 4 on the right. The quantity $\partial \delta_s / \partial \delta_u$ is changing in the investigated range of δ_u and r_1-R_1 between about 2 [-] and about 14 [-].

8. Conclusions

For the investigated SV:

- The absolute armature eccentricity is almost independent of the thickness of the sleeve. However for the hydraulic clearance equal to 10 µm, the minimum distance from the armature side surface to the inner sleeve surface of about 0.1 µm is bigger for the sleeve thickness equal to 290 µm than for the sleeve thickness equal to 140 µm. The variation of this distance is equal to about 20 % of the roughness of the contact armature-sleeve.

- The minimum distance from the armature side surface to the inner sleeve surface varies from about 1 µm to about 1.5 µm. It means that this distance is twice to three times bigger that the roughness of the contact armature-sleeve.

Appendix A: Excerpt from integral tables [16]

The integral (A 1) is to be found

$$J_2^{01} = \left[I_2^{01} \right]_0^{2\pi} = \int_0^{2\pi} \left(1 - \varepsilon \cos\sigma \right)^{-2} \cos\sigma \, \mathrm{d}\sigma \,. \tag{A 1}$$

The indefinite integral I_2^{01} is equal to

$$I_2^{01} = -\varepsilon^{-1} \left(-I_2^{00} + I_1^{00} \right). \tag{A 2}$$

For the first term of (A 2) can be written

$$I_2^{00} = \left(1 - \varepsilon^2 \right)^{-1} \left(-\varepsilon \left(1 - \varepsilon\cos\sigma \right)^{-1} \sin\sigma + I_1^{00} \right). \tag{A 3}$$

The setting of (A 3) in (A 2) yields

$$I_2^{01} = -\varepsilon^{-1} \left(1 - \varepsilon^2 \right)^{-1} \varepsilon \left(1 - \varepsilon\cos\sigma \right)^{-1} \sin\sigma + \varepsilon \left(1 - \varepsilon^2 \right)^{-1} I_1^{00} \,. \tag{A 4}$$

The definite integral of the first term of (A 4) in boundaries $[0, 2\pi]$ is equal zero. For the definite integral of the second term of (A 4) one obtains from [16]

$$\left[I_2^{00} \right]_0^{2\pi} = 2\pi \left(1 - \varepsilon^2 \right)^{-1/2} \,. \tag{A 5}$$

The setting of (A 5) in (A 4) results in

$$J_2^{01} = 2\pi\varepsilon \left(1 - \varepsilon^2 \right)^{-3/2} \,. \tag{A 6}$$
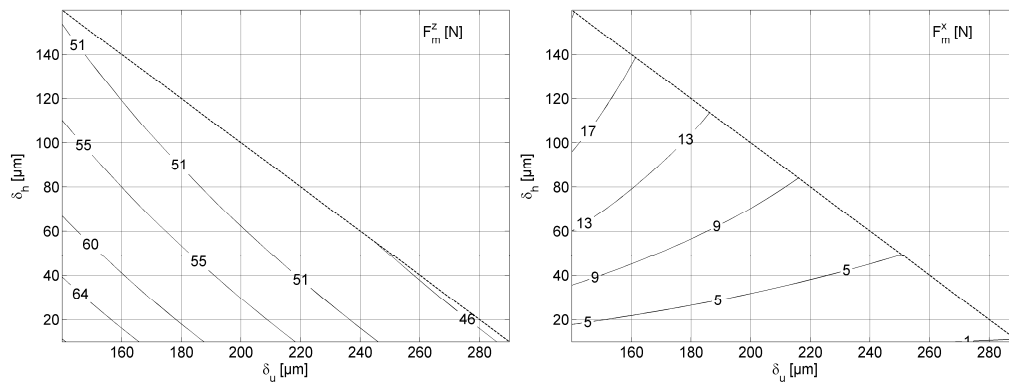
Appendix B: Additional calculation results

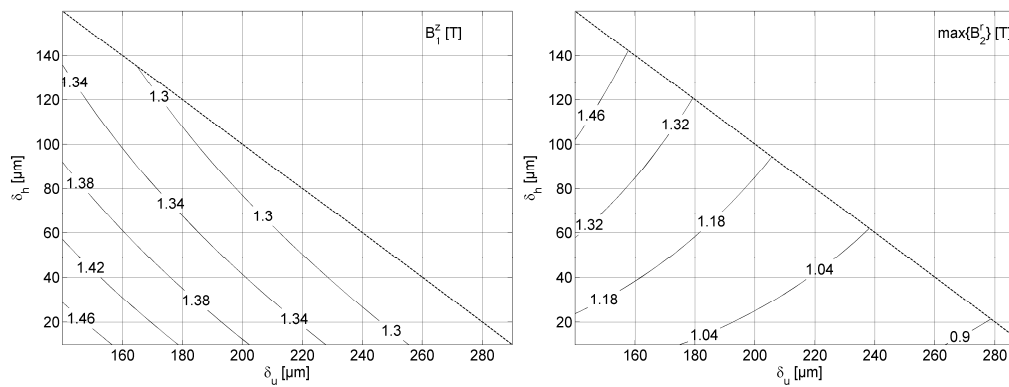Fig. 5. Axial (left) and transversal component of the magnetic force acting on the armature

Fig. 6. Axial magnetic flux density (left) and maximal value of transversal component
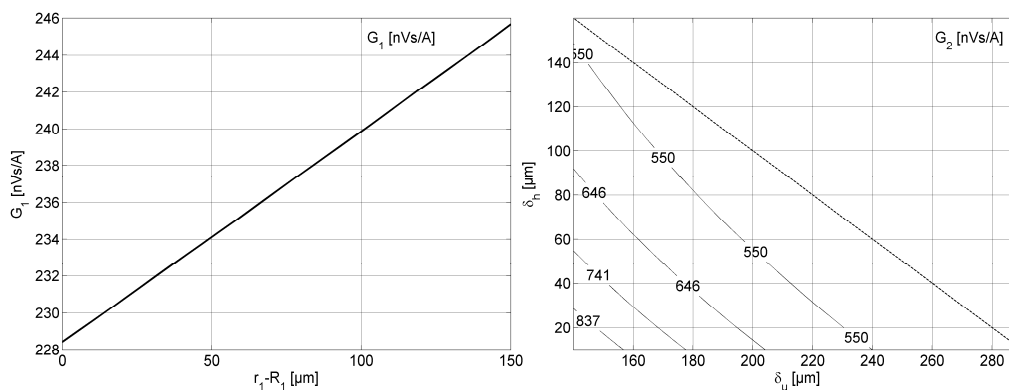of the magnetic flux density

Fig. 7. Magnetic permeance of the axial (left) and radial air gap

References

[1] Bottauscio O., Chiampi M., Manzin A., *Different finite element approaches for electromechanical dynamics,* IEEE Transactions on Magnetics 40(2): 541-544 (2004).

[2] Huber B., Ulbrich H., *Modeling and experimental validation of the solenoid valve of a common rail diesel injector*, SAE Technical Paper 2014-01-0195 (2014).

[3] Shahroudi K., Peterson D., Belt D., I*ndirect adaptive closed loop control of solenoid actuated gas and liquid injection valves,* SAE Technical Paper 2006-01-0007 (2006).

[4] Lu F., Deng J., Hu Z., I*mpact of control methods on dynamic characteristic of high speed solenoid injectors*, SAE Technical Paper 2014-01-1445 (2014).

[5] Angadi S. V., Jackson S., Choe S., *Reliability and life study of hydraulic solenoid valve. Part 1: a multi-physics finite element model*, Engineering Failure Analysis 16(3): 874-887 (2009).

[6] Peng L., Liyun F., Qaisar H., De X., Xiuzhen M., Enzhe S., *Research on Key factors and their interaction effects of electromagnetic force of high-speed solenoid valve,* The Scientific World Journal. Hindawi Publishing Corporation.*,* Article ID 567242 (2014).

[7] Vogel R., *Numerische Berechnung der Ankerreibung eines elektromagnetischen Schaltventils. Studienarbeit*, Universität Dortmund, Dortmund (2006).

[8] Deland D. L., *Solenoid arrangement with segmented armature member for reducing radial force*, Davison, MI (US) Patent US 8,421,568 B2 (2013).

[9] Goraj R., *Elektromagnetisches Schaltventil,* Germany Patent DE 10 2007 023 363 A1 (2007).

[10] Kleist A., *Berechnung von Dicht- und Lagerfugen in hydrostatischen Maschinen, Shaker Verlag*, Aachen (2002).

[11] Kallenbach E., *Elektromagnete-Grundlagen, Berechnung, Entwurf und Anwendung,* Teubner Verlag/ GWV Fachverlage GmbH, Wiesbach (2003).

[12] Getzlaff M., *Fundamentals of magnetism*, Springer, Berlin, Heidelberg (2008).

[13] Küpfmüller K., Kohn G., *Theoretische Elektrotechnik und Elektronik*, Springer Berlin (1993).

[14] Stefanita C. G., *Magnetism, basics and applications*, Springer, Berlin, Heidelberg (2012).

[15] Rawa H., *Electricity and magnetism in technology (in Polish),* Wydawnictwo Naukowe PWN, Warszawa (2001).

[16] Booker J. F., *A table of the journal-bearing integral,* Journal of Basic Engineering 87(2): 533-535 (1965).

[17] Greenwood J., Williamson J., *Contact of nominally flat surfaces,* Proc. Royal Soc. London*,* 295(1442): 300-319 (1966).